1.E.3:
2.B

Nuclear Physics **A315** (1979) 133–142;

TRANSIENT FIELD *g*-FACTOR MEASUREMENTS ON THE 2_1^+ STATES OF ^{32}S AND ^{34}S

P. C. ZALM [†], A. HOLTHUIZEN, J. A. G. DE RAEDT and G. VAN MIDDELKOOP
Fysisch Laboratorium, Rijksuniversiteit, Utrecht, The Netherlands

Received 8 February 1978
(Revised 9 October 1978)

Abstract: Transient field integral precession measurements have been performed on the first-excited $J^\pi = 2^+$ states of ^{32}S and ^{34}S with the IMPAC technique on recoil into magnetized iron single-crystal frames. The results were analysed with an empirical parametrization of the field. This yields *g*-factors of $g = +0.47 \pm 0.09$ and $+0.50 \pm 0.08$ for ^{32}S and ^{34}S, respectively. In the present cases the influence of static magnetic hyperfine fields is negligible due to the short mean lives for ^{32}S and ^{34}S of 0.23 and 0.46 ps, respectively. Various complex model calculations yield *g*-factors in good agreement with experiment. Measured *g*-factors, including the present data, for light self-conjugate and neutron-excess $T_z = 1$ nuclei are also briefly discussed. The measured value of the *g*-factor for ^{32}S confirms the empirical description of the transient field.

E

NUCLEAR REACTIONS ^{32}S$(\alpha, \alpha'\gamma)$, $E = 8.25$ MeV; ^{34}S$(\alpha, \alpha'\gamma)$, $E = 8.90$ MeV; measured $\alpha\gamma(\theta, B)$ in polarized Fe. ^{32,34}S levels deduced g for first 2^+ states. ^{34}S enriched target. IMPAC.

1. Introduction

The transient magnetic field experienced by a nucleus slowing down in magnetized Fe is currently explained by a transfer of polarized electrons from the ferromagnetic host into bound atomic s-shells of the moving nuclear ion [1-3]. It has been shown [2]) that this field can be parametrized as a (saw-tooth like) function of atomic number and as a (linear) function of recoil velocity of the moving ion. For nuclei with $Z \leqq 14$ this parametrization yields a calibration which reproduces the measured field strength to within 5 %. It is expected that this calibration is still good for $Z < 20$. This enables one to perform *g*-factor measurements in this region on short-lived ($\tau = 0.1$–10 ps) excited states by the transient field implantation perturbed angular correlation (TF-IMPAC) technique. For states with lifetimes greater than the stopping time in Fe one can avoid contributions from the often not well-known static hyperfine fields by taking the ferromagnetic medium thin enough such that the nuclei recoil through

† Present address: Philips' Natuurkundig Laboratorium, Eindhoven, The Netherlands.

this medium and stop in non-ferromagnetic material [4]). In this paper we report on g-factor measurements for the first-excited 2^+ states of ^{32}S and ^{34}S.

The investigation of these even sulphur isotopes is an extension of a series of g-factor measurements on first-excited 2^+ states in selfconjugate ($T_z = 0$) and neutron-excess ($T_z = +1$) even-even nuclei in the sd shell, Ne, Mg and Si, carried out so far in this laboratory [5-8]). The lifetimes of the S-states (0.23 ps for ^{32}S and 0.46 ps for ^{34}S; see subsect. 3.2) are sufficiently short in comparison to the stopping time for S-ions in Fe with initial velocities of $v_i \approx 1.5v_0$ ($v_0 = \frac{1}{137}c$) such that the contribution of the (unknown) static field to the measured integral spin precessions is negligible.

It will be shown that the g-factors of light $T_z = +1$ nuclei exhibit a highly individual character and do not follow the complex-state estimate $g = Z/A$. Although the presently obtained g-factor for ^{34}S is close to Z/A and close to practically all theoretically predicted values, this is certainly not a general feature of $T_z = +1$ states as has been shown for ^{22}Ne [ref. [8])], ^{26}Mg and ^{30}Si [refs. [2,6])].

It may be worth noting, finally, that the measurement of a pair of g-factors in isotopes of the same element, one of which is an even-even $T_z = 0$ nucleus, yields simultaneously information on a $T_z \neq 0$ state and on the transient field strength. The g-factor of the $T_z = 0$ state, in the present case $^{32}S(2_1^+)$, is reliably estimated from systematics [9]) to be 0.5 to within 10 %. Hence a TF-IMPAC measurement of this g-factor also provides an extension and a test of the transient field calibration obtained in ref. [2]).

2. Experimental procedure

The 2.23 and 2.13 MeV levels of ^{32}S and ^{34}S, respectively, were excited by inelastic scattering of α-particles obtained from the Utrecht 7 MV EN tandem accelerator. The experimental set-up with a single-crystal Fe window frame as a target backing [10]), and the associated data collecting system have been described in detail elsewhere [5,7]).

Targets of about 200 $\mu g/cm^2$ ZnS were prepared by vacuum evaporation on the Fe single-crystal frame. The thicknesses were determined both by weighing of a sample which was prepared simultaneously under identical conditions and by comparing the coincident γ-ray yields with those of accurately weighed ZnS targets on thin formvar backings. For the ^{32}S experiment a natural ZnS target (i.e. the sulphur is 95 % ^{32}S) and for the ^{34}S experiment $Zn^{34}S$ enriched to 90 % in ^{34}S were used.

The coincident yields and γ-ray anisotropies for the (α, α') reactions were first measured as a function of the $^4He^{++}$ bombarding energy. Outgoing α-particles were detected at 180° with respect to the beam direction, in coincidence with γ-rays detected in NaI(Tl) counters at 45° and 90°. The bombarding energies ranged from just above the Coulomb barrier (7.0 MeV) to about 12 MeV. Higher energies had to be discarded because of the prolific background due to reactions in the thick iron backing. The optimum α-particle bombarding energies for the integral precession measurements

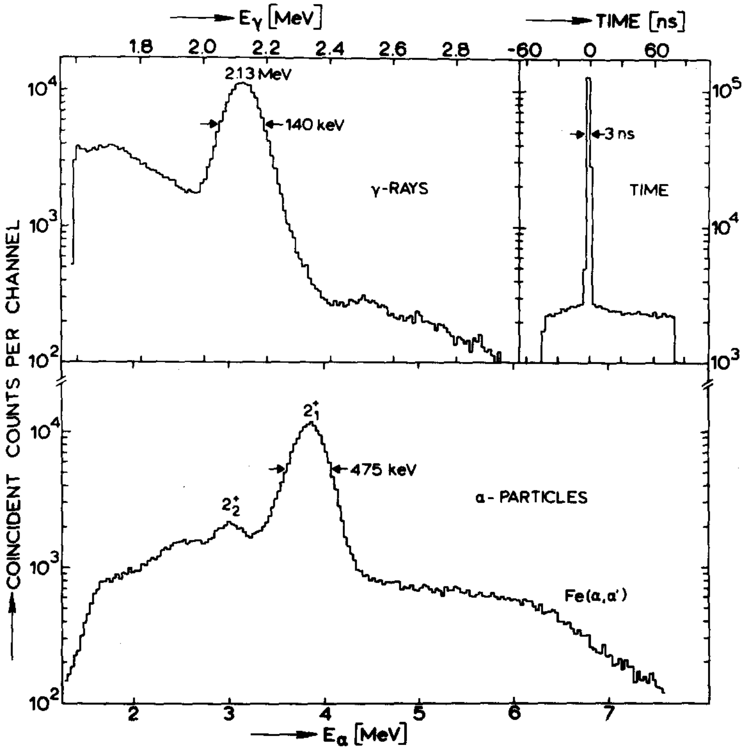

Fig. 1. Typical coincident α-particle, γ-ray and time spectra for ^{34}S. The spectra were generated with windows set on the respective peaks. No random background has been subtracted.

were found to be 8.25 MeV for ^{32}S and 8.90 MeV for ^{34}S. At these energies, well below the Coulomb barrier for Zn (10.5 MeV), the background from reactions with Zn isotopes was negligible (see also fig. 1).

Coincident γ-radiation was detected by six 12.7 cm diameter by 12.7 cm long NaI(Tl) detectors at angles $\frac{1}{2}\pi(n \pm \frac{1}{3})$, with $n = 0, \pm 1$. The γ-ray energies corresponding to the first-excited states of ^{32}S and ^{34}S cannot be resolved by these γ-ray counters. Therefore in addition a large-volume Ge(Li) detector was positioned at 0° to the beam direction to monitor the relative contribution of ^{32}S coincident γ-rays in the ^{34}S experiment. This contribution was found to be less than 3 %. From the yield measurements it was calculated that in the ^{32}S experiment at $E_\alpha = 8.25$ MeV the contribution of ^{34}S γ-rays to the photopeak of the 2.23 MeV γ-ray in ^{32}S was less than 1 %.

The single-crystal frame was magnetized by a current of 0.8 A through a 60 turn coil on one of the legs, corresponding to a magnetizing field of about 15 G (1200 A/m). The direction of this field was reversed automatically every 2 min. In order to maintain good true-to-random coincidence ratios, to limit pulse pile-up and dead-time losses and to prevent heating of the frame, the beam current (typically 70 nA for ^{32}S and 55 nA for ^{34}S) was not allowed to exceed 80 nA ($^4He^{++}$).

The total background-subtracted yield obtained in the photopeak for ^{32}S was 2.4×10^5 counts per detector for each field direction and 1.4×10^5 for ^{34}S. The measurements required a beam time of 100 h each. The quality of the data obtained for e.g. ^{34}S can be inferred from the coincident α-particle, γ-ray and time spectra displayed in fig. 1.

3. Statistical considerations, analysis and results

3.1. STATISTICS

For small rotations the mean integral precession angle $\Delta\theta$ can be expressed as

$$\Delta\theta = \frac{\sqrt{r}-1}{\sqrt{r}+1} \Big/ \frac{1}{W(\theta)} \frac{\mathrm{d}W(\theta)}{\mathrm{d}\theta}, \tag{1}$$

where $W(\theta)$ represents the γ-ray angular correlation. The double ratio r and the corresponding effect ε are defined by

$$r = 1+\varepsilon = \frac{N[\frac{1}{2}\pi(n+\frac{1}{5})]_\uparrow N[\frac{1}{2}\pi(n-\frac{1}{5})]_\downarrow}{N[\frac{1}{2}\pi(n+\frac{1}{5})]_\downarrow N[\frac{1}{2}\pi(n-\frac{1}{5})]_\uparrow}, \tag{2}$$

where $N[\phi]_{\uparrow\downarrow}$ denotes the number of coincident counts accumulated in the γ-ray detector at angle ϕ with magnetic field up or down. For the four γ-ray detectors at $\pm 72°$ and $\pm 108°$, the cross-effects ε_c, given by

$$\varepsilon_c = \frac{N[\frac{1}{2}\pi(1\pm\frac{1}{5})]_\uparrow N[-\frac{1}{2}\pi(1\mp\frac{1}{5})]_\downarrow}{N[\frac{1}{2}\pi(1\pm\frac{1}{5})]_\downarrow N[-\frac{1}{2}\pi(1\mp\frac{1}{5})]_\uparrow} - 1, \tag{3}$$

which should be zero, can be used as a check on the measurement.

The logarithmic derivative $W^{-1}\,\mathrm{d}W/\mathrm{d}\theta$ of the γ-ray angular correlation function $W(\theta)$, i.e. the calibration of the double ratio r against rotation angle, was obtained by measuring ε for a rotation of 2°. This was performed by off-setting the six-counter array by angles $\pm 2°$ with the magnetic field switched off.

The observed effects ε as well as the cross-effects ε_c are summarized in table 1 together with the $W^{-1}\,\mathrm{d}W/\mathrm{d}\theta$ calibration. The results for the detector pairs at $\pm 72°$ and $\pm 108°$ (first line for each isotope) have been averaged. For the detector pair at $\pm 18°$ (second line for each isotope) the results are given separately since here the logarithmic derivative of $W(\theta)$ is different from those at $\pm 72°$ and $\pm 108°$ due to the finite solid angles of the γ-ray counters. For these two counters no cross-effects can be given. The mean integral precession angles $\Delta\theta$ deduced from the data are also included in table 1.

Frequency distributions of the effects and cross-effects per recorded magnetic tape (70 min for ^{32}S and 100 min for ^{34}S) served as a check on the data. No significant deviations from a Gaussian distribution were observed (see fig. 2). To investigate the

TABLE 1

Summary of the measured effects [a]) and deduced precessions for ^{32}S and ^{34}S

Nucleus	Precession in Fe		Calibration $\pm 2°$ off-set [b])		$\Delta\theta$ (mrad)
	ε (%)	ε_c (%)	ε (%)	ε_c (%)	
^{32}S	1.69 ± 0.33 1.70 ± 0.41	-0.16 ± 0.33	79 ± 2 67 ± 3	1 ± 2	1.06 ± 0.18
^{34}S	3.00 ± 0.45 1.92 ± 0.60	0.20 ± 0.45	73 ± 2 54 ± 3	2 ± 3	1.80 ± 0.25

[a]) The results of the detector pairs at $\pm 72°$ and $\pm 108°$ have been averaged.
[b]) See text.

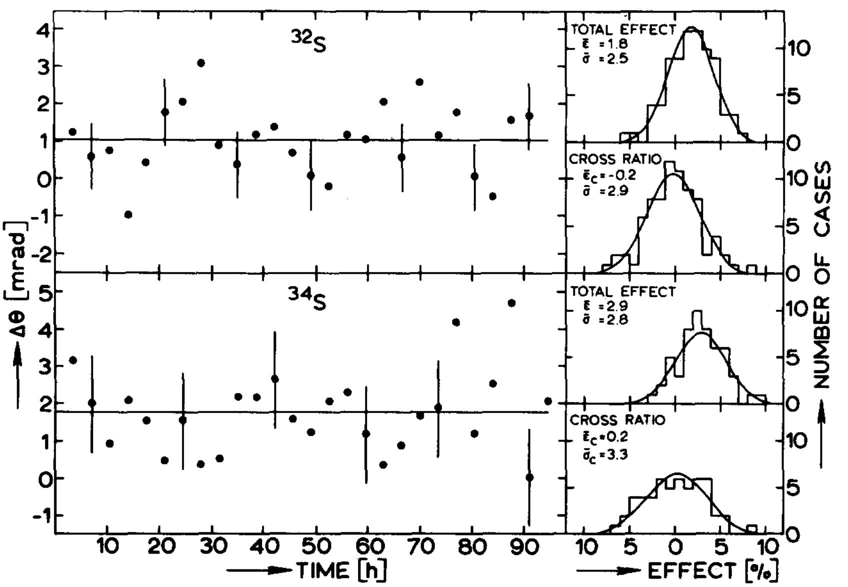

Fig. 2. The measured rotation angles $\Delta\theta$ per run of 3.5 h as a function of time. The solid lines represent the average value. Frequency distributions of the precession effects ε and cross effects ε_c per recorded magnetic tape are also shown. The results of the detector pair at $\pm 18°$ have been scaled by the $W^{-1}dW/d\theta$ calibration and averaged with the results of the pairs at $\pm 72°$ and $\pm 108°$. The expected Gaussian distributions are indicated.

possibility of building up radiation damage in the ferromagnetic backing the experiments were divided into runs of about 3.5 h and the mean precession angle per run was calculated. The results are displayed in fig. 2. There is no significant decrease of the rotation with time. A least-squares fit of a linear function to the data yields a slope of $(0 \pm 6) \times 10^{-3}$ and $(8 \pm 6) \times 10^{-3}$ mrad/h for ^{32}S and ^{34}S, respectively.

3.2. THE g-FACTORS

The experimentally observed integral precession angles were interpreted with the transient field dependence on recoil velocity and atomic number as obtained in ref. [2]. The field, assumed to be due to unpaired polarized 2s electrons of the moving ion, is given by

$$B_{\mathrm{TF}}(v, Z) = C(Z)v/v_0. \tag{4}$$

The integral transient-field precession angle per g was calculated from the expression

$$\frac{\Delta\theta}{g} = \frac{\mu_N}{\hbar\tau}\int_0^\infty \left[\int_0^{t'} B_{\mathrm{TF}}(t)\mathrm{d}t\right] \exp\left[-(t'+t_i)/\tau\right]\mathrm{d}t', \tag{5}$$

where t_i is the average time that has elapsed before the recoiling ions enter the ferromagnetic backing. The conversion from velocity v to time t is obtained from the electronic and nuclear stopping powers $\mathrm{d}E/\mathrm{d}x$ (see below). The initial time t_i equals the time necessary for the ions to travel half the target thickness; it is calculated from the stopping powers in the target material. Eq. (5) was evaluated numerically by a computer program in order to calculate the g-factors and the error propagation.

In order to envisage the relative importance of the various parameters in the calculation of $\Delta\theta/g$ it is useful to evaluate eq. (5) with the *approximation* that

$$\frac{\mathrm{d}E}{\mathrm{d}x} = -k\sqrt{E},$$

hence $v(t) = v_i \exp(-t/\tau_s)$, where τ_s is the mean slowing-down time. This leads to the expression

$$\frac{\Delta\theta}{g} = 0.048C(Z)\frac{v_i}{v_0}\exp(-t_i/\tau)\frac{\tau\tau_s}{\tau+\tau_s} \qquad [\mathrm{mrad}], \tag{7}$$

where the index i labels the initial conditions and $C(Z)$ and τ are given in [T] and [ps], respectively. Although this approximation is not valid at very low and high recoil energies it leads to quite accurate results. It was found that, upon evaluating τ_s at $E \approx 0.4E_i$, for initial recoil energies between 0.1 and 1 MeV/amu for nuclei with mass $10 < A < 40$, the integral precessions in iron obtained from eq. (7) differ by less than 10 % from those calculated through eq. (5) with accurate stopping power data. For the present experiments on sulphur one has $\tau_s = 0.3$ ps.

The resulting relative errors in the g-factors computed through eq. (5) are given in table 2. The contributions of the uncertainties in each quantity to the total error are also shown; they will be discussed in some detail below.

(*i*) *Static field* B_s. As mentioned in sect. 1 the static magnetic field acting on the sulphur ions after they have come to rest in the iron lattice is not known. An estimate may be obtained by taking the systematic trend of the fields in series of elements with similar electron configurations, e.g. In and following elements, and scaling this to the known fields of the nearby elements Al and P in Fe [ref. [11]]. This leads to

TABLE 2

Sources of errors and their contribution to the error in the g-factors

Quantity [a]	^{32}S		^{34}S	
	relative error (%)	contribution to g (%)	relative error (%)	contribution to g (%)
$\Delta\theta$	17	17	14	14
B_s	100	0	100	1
τ	7	6	5	3
dE/dx	5	2	5	3
d	10	4	10	2
$C(16)$	4	4	4	4
	total error	19	total error	15

[a]) The symbols are explained in the text.

the conclusion that the static field must be smaller than 10 T, which gives rise to a correction for ^{34}S of at most 1 %. For ^{32}S the static field contribution is even a factor of five smaller.

(*ii*) *Mean lives* τ. The values for the mean lives of the ^{32}S and ^{34}S first-excited states are 230 ± 16 fs and 460 ± 23 fs, respectively [12, 15]). Since the lifetimes are shorter than the stopping time, which is approximately 0.6 ps ($2\tau_s$), the uncertainty in the calculated precessions due to errors in τ is appreciable [see eq. (7) and table 2].

(*iii*) *Stopping power* dE/dx. Electronic stopping powers in Fe interpolated from the tabulation of Northcliffe and Schilling [13]) were scaled by recent data from Ward *et al.* [14]) on the stopping of α-particles. The uncertainty in the electronic stopping powers thus obtained is estimated to be at most 5 %. For details about this scaling procedure, as applied in lifetime measurements with the Doppler-shift attenuation method, the reader is referred to ref. [15]). For the nuclear stopping power the universal function of Kalbitzer *et al.* [16]) was taken with an adopted uncertainty of 25 %. The approximate contribution of the uncertainty in the electronic stopping power on $\Delta\theta/g$ can easily be interferred from eq. (7). Nuclear stopping is important only at low velocity, i.e. where the field is small, and hence will not influence the result significantly, especially for lifetimes (appreciably) shorter than the stopping time.

(*iv*) *Target thickness d*. The two independent thickness estimates discussed in sect. 2 agree with each other to within 15 %, which leads to an estimated uncertainty of about 10 %. The target thickness affects the entrance parameters v_i and t_i, the latter of which is most sensitive to thickness variations.

(*v*) *Z-dependence of the field C(16)*. The constant $C(Z = 16)$ was calculated from the systematics described in ref. [2]). This leads to $C(16) = 281 \pm 11$ T.

The errors are treated independently and yield relative errors in the values of the g-factors for ^{32}S and ^{34}S of 19 % and 15 %, respectively. This leads to the final results for ^{32}S(2_1^+) and ^{34}S(2_1^+) of $g = +0.47 \pm 0.09$ and $g = +0.50 \pm 0.08$, respectively.

4. Comparison with theory and conclusion

The experimental values for the g-factors of the first-excited 2^+ states of ^{32}S and ^{34}S are compared with several theoretical predictions in table 3. The calculations are specified in some detail below.

TABLE 3

Comparison of theoretical g-factors with experiment

		^{32}S	^{34}S
Experiment		$+0.47 \pm 0.09$	$+0.50 \pm 0.08$
Theory [a]):	PHF [b])	$+0.53$	
	MSDI [c])	$+0.51$	$+0.54$
	ASDI [d])	$+0.49$	
	CW [e])	$+0.50$; $+0.53$	$+0.43$; $+0.50$
	pure conf. [f])	$+0.54$	$+0.77$
	Z/A	$+0.50$	$+0.47$

[a]) The abbreviations are explained in the text.

[b]) Ref. [17]). [c]) Ref. [18]). [d]) Ref. [19]).

[e]) Ref. [20]); the first and second value correspond to calculations with bare and effective nucleon g-factors, respectively.

[f]) Pure $2s_{1/2}^{-1}d_{3/2}$ and $\nu d_{3/2}^{2}$ configurations for ^{32}S and ^{34}S, respectively.

(*i*) *PHF.* A projected Hartree-Fock calculation with the lowest five major oscillator shells as model space [17]).

(*ii*) *MSDI.* A shell-model calculation [18]) in a $1d_{\frac{5}{2}}2s_{\frac{1}{2}}1d_{\frac{3}{2}}$ configuration space with a maximum of two holes in the $1d_{\frac{5}{2}}$ orbit. The modified surface-delta interaction is taken as effective two-body interaction.

(*iii*) *ASDI.* A sd shell-model calculation [19]) with an "adjusted surface-delta interaction". The configuration space is truncated with the diagonal energy truncation method.

(*iv*) *CW.* A full sd space shell-model calculation by Chung and Wildenthal [20]). The 63 two-body matrix elements and 3 single-particle orbital energies were fitted to low-lying positive parity levels in $A = 32$–39 nuclei. Results with bare and effective single-particle spin and orbital g-factors are given. The latter allegedly give better agreement.

(*v*) For the sake of completeness the pure configuration estimates $2s_{\frac{1}{2}}^{-1}1d_{\frac{3}{2}}$ and $\nu d_{\frac{3}{2}}^{2}$ for ^{32}S and ^{34}S, respectively, and the rotational model (or random-state) estimates $g = Z/A$ are also included.

As mentioned before, the g-factors of low-lying states of even-even selfconjugate nuclei are expected to be close to $g = +0.5$ [ref. [9])]. This rule has been experimentally verified for a number of light nuclei, including ^{32}S from the present work; see the lower part of fig. 3. For these cases one therefore does not expect the computed (isoscalar) g-factors to depend very much on the assumed interaction or configuration

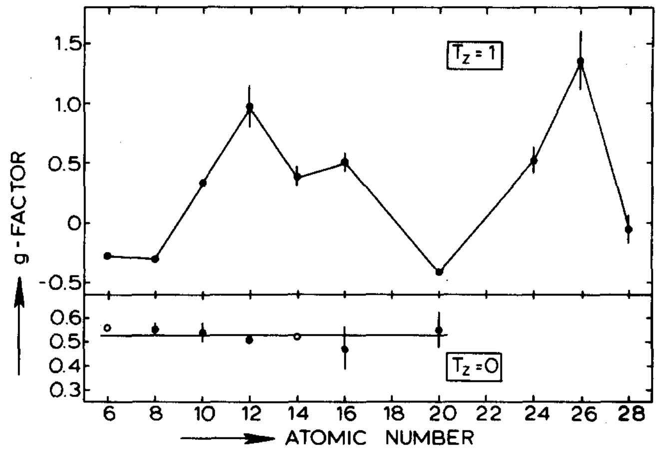

Fig. 3. A summary of measured g-factors of low-lying states in self-conjugate ($N = Z$; $T_z = 0$) and neutron excess ($N = Z+2$; $T_z = 1$) even-even nuclei. The two values indicated with open circles are from transient field measurements, which were also used to obtain the field calibration. These values are consistent with the empirical description of the transient field. The data were taken from refs. [2,4,6-8,21,22]).

space. This is clearly demonstrated by the small spread in computed values for ^{32}S in table 3.

For even-even $T_z = +1$ nuclei, however, no such simple rule can be formulated. The measured values for the g-factors vary between $g = -0.4$ and $g = +1.4$ for $Z \leqq 28$ (see upper part of fig. 3) indicating large variations in the isovector part of the g-factor. In these cases the computed values do sometimes depend sensitively on the interaction or configuration space used [see e.g. refs. [6,8])]. For ^{34}S, however, all complex model predictions are very close to the experimental value. This means that for this particular case the g-factor is not a sensitive probe for the wave function. Only the crude estimate for a pure f^n configuration shows that the wave function is more complex than the simplest possible one.

The fact that for ^{32}S the g-factor must be close to 0.5 enables us to use the present measurements also as a check on the empirical transient field calibration. With the assumption $g(^{32}S) = 0.50 \pm 0.05$ one obtains for the field strength $C(16) = 260 \pm 50$ T, in good agreement with the extrapolated calibration which yields $C(16) = 281 \pm 11$ T (see subsect. 3.2).

The authors like to thank Dr. W. A. Sterrenburg and A. J. Rutten for their valuable help during the experiments. This work was performed as part of the research program of the "Stichting voor Fundamenteel Onderzoek der Materie" (FOM) with financial support from the "Nederlandse Organisatie voor Zuiver-Wetenschappelijk Onderzoek" (ZWO).

References

1) J. L. Eberhardt, R. E. Horstman, P. C. Zalm, H. A. Doubt and G. van Middelkoop, Hyperfine Interactions **3** (1977) 195
2) P. C. Zalm, A. Holthuizen, J. A. G. De Raedt and G. van Middelkoop, Phys. Lett. **69B** (1977) 157; Hyperfine Interactions **5** (1978) 347
3) G. van Middelkoop, J. A. G. De Raedt, A. Holthuizen, W. A. Sterrenburg and R. Kalish, Phys. Rev. Lett. **40** (1978) 24
4) J. M. Brennan, N. Benczer-Koller, M. Hass and H. T. King, Phys. Rev. **C16** (1977) 899
5) J. L. Eberhardt, R. E. Horstman, H. W. Heeman and G. van Middelkoop, Nucl. Phys. **A229** (1974) 162
6) J. L. Eberhardt, R. E. Horstman, H. A. Doubt and G. van Middelkoop, Nucl. Phys. **A244** (1975) 1
7) R. E. Horstman, J. L. Eberhardt, H. A. Doubt, C. M. E. Otten and G. van Middelkoop, Nucl. Phys. **A248** (1975) 291
8) R. E. Horstman, J. L. Eberhardt, P. C. Zalm, H. A. Doubt and G. van Middelkoop, Nucl. Phys. **A275** (1977) 237
9) J. F. A. van Hienen and P. W. M. Glaudemans, Phys. Lett. **42B** (1972) 301;
P. C. Zalm, J. F. A. van Hienen and P. W. M. Glaudemans, Z. Phys. **A287** (1978) 255
10) P. C. Zalm, J. L. Eberhardt, R. E. Horstman, G. van Middelkoop and H. de Waard, Phys. Lett. **60B** (1976) 258 and Nucl. Instr., submitted
11) G. N. Rao, Atomic Data and Nucl. Data Tables **15** (1975) 553
12) P. M. Endt and C. van der Leun, Nucl. Phys. **A214** (1973) 1;
D. Schwalm, E. K. Warburton and J. W. Olness, Nucl. Phys. **A293** (1977) 425
13) L. C. Northcliffe and R. F. Schilling, Nucl. Data Tables **7** (1970) 223
14) D. Ward, J. S. Forster, H. R. Andrews, I. V. Mitchell, G. C. Ball, W. G. Davies and G. J. Costa, Atomic Energy of Canada report AECL-5313 (1976)
15) J. A. J. Hermans, G. A. P. Engelbertink, L. P. Ekström, H. H. Eggenhuisen and M. A. van Driel, Nucl. Phys. **A284** (1977) 307
16) S. Kalbitzer, H. Oetzmann, H. Grahmann and A. Feuerstein, Z. Phys. **A278** (1976) 223
17) M. R. Guyne, Phys. Lett. **37B** (1971) 125
18) P. W. M. Glaudemans, P. M. Endt and A. E. L. Dieperink, Ann. of Phys. **63** (1971) 134
19) F. E. H. van Eijkern, G. A. Timmer, F. Meurders and P. W. M. Glaudemans, Z. Phys. **A278** (1976) 337
20) W. Chung and B. H. Wildenthal, to be published;
W. Chung, Ph.D. thesis, Michigan State University (1976)
21) V. S. Shirley and C. M. Lederer, Hyperfine interactions studied in nuclear reactions and decay, ed. E. Karlsson and R. Wäppling (Almqvist & Wiksell, Stockholm, 1975) p. 1
22) J. Asher, M. A. Grace, P. D. Johnston, J. W. Koen, P. M. Rowe and W. L. Randolph, J. of Phys. **G2** (1976) 477;
C. Fahlander, K. Johansson, E. Karlsson and G. Possnert, Nucl. Phys. **A291** (1977) 241;
J. M. Brennan, N. Benczer-Koller, M. Hass and H. T. King, Hyperfine Interactions **4** (1978) 268